An Online Trajectory Tracking Control of a Double Flexible Joint Manipulator Robot by Considering the Parametric and Non-Parametric Uncertainty

Alireza Pezhman[1], Javad Rezapour [2,*]
Department of Mechanical Engineering,
Lahijan Branch,Islamic Azad University, Lahijan, Iran,
E-mail: pezhmanalireza37@gmail.com & Rezapour@liau.ac.ir
*Corresponding author

Mohammad Javad Mahmoodabadi [3]
Department of Mechanical Engineering,
Sirjan University of Technology, Sirjan, Iran,
E-mail: mahmoodabadi@sirjantech.ac.ir

Received: 11 October 2020, Revised: 8 February 2021, Accepted: 11 February 2021

Abstract: Accurate trajectory tracking and control of the Double Flexible Joint Manipulator lead to design a controller with complex features. In this paper, we study two significant strategies based on improving the structure of the hybrid controller and training the controller parameters for an online estimation of time-varying parametric uncertainities. For this purpose, combination of feedback linearization with an adaptive sliding mode control by considering update mechanism is utilized to stabilize the DFJM system. The update mechanism is obtained based on gradient descend method and chain rule of the derivation. Following, in order to eliminate the tedious trial-and-error process of determining the control coefficients, an evolutionary algorithm (NSGA-II) is used to extract the optimal parameters by minimizing the tracking error and control input. In the second step, an online estimation of the designed parameters were proposed based on three intelligent methods; weighting function, Adaptive Neural Network Function Fitting (ANNF), and adaptive Neuro-fuzzy inference system (ANFIS-PSO). The proposed controller reliability finally was examined in condition of the mass and the length of the robot arm was changed and sudden disturbances were imposed at the moment of equilibrium position, simultanously. The results of the tracking error and control input of the trained proposed controller demonstrated minimal energy consumption and shorter stability time in condition that the control parameters are constant and training are not considered.

Keywords: Double Flexible Joint Manipulator, Gradient Descent Method, Sliding Mode Controller, Uncertainy

How to cite this paper: Ali Reza Pezhman, Javad Rezapour, and Mohammad Javad Mahmooabadi, "An Online Trajectory Tracking Control of a Double Flexible Joint Manipulator Robot by Considering the Parametric and Non-Parametric Uncertainty" , Int J of Advanced Design and Manufacturing Technology, Vol. 14/No. 2, 2021, pp. 93–110. DOI: 10.30495/admt.2021.1911965.1223

Biographical notes: Alireza Pezhman is a PhD student of Lahijan Islamic Azad University, Iran in the same field. **Javad Rezapour** received his BSc, MSc and the PhD degrees in Mechanical Engineering from Guilan University, Rasht, Iran, in 2007, 2009 and 2015, respectively. He is currently an assistant professor of Control Engineering in Islamic Azad University of Lahijan. **Mohammad Javad Mahmoodabadi** received his BSc, MSc and PhD at Mechanical Engineering from Shahid Bahonar University of Kerman and Guilan University, Iran in 2005, 2007 and 2012 respectively. Now, he is an Associate Professor of Mechanical Engineering in the Sirjan University of Technology, Sirjan, Iran.

1 INTRODUCTION

Flexible links are one of the most important, difficult and complex issues in the field of robotics. These links, due to lower weight and reduced inertia, have a faster performance and lower energy consumption than rigid links. With these desirable features, the flexibility of these links increases the complexity of their control and tracking, which provides a new field of research in designing and controlling the robot link trajectory with an acceptable accuracy. In ordinary robots, controlling the end of the assembled link is equivalent to rigid mode control. However, for optimum control of the flexible link, it is necessary to have a more reliable controller over the inflexible conditions in order to take into consideration the inevitable vibrations and oscillations.
Different methods were used to control the FJM such as observation method that estimates the velocity of each link and motor rotor by a dynamic output feedback controller and robust trajectory tracking control for rigid and flexible link manipulators based on estimation of uncertainty and disturbance [1-2]. For example, Control of rotary flexible link is proposed by concentrating on Linear Quadratic Regulator (LQR) and exponential tracking control by using back stepping approach for voltage-based control of a flexible joint [3-4]. Furthermore, a new robust control procedure was introduced for robot manipulators based on combination of coefficient diagram method controllers and back stepping to create a novel control law [5-6]. Likewise, Qinxuan et al. [7] investigated an active control of space manipulator with flexible-link and flexible joint based on the singular perturbation method. A singular pertubation theory concerns on problems containing a small parameter that cannot be approximated by setting the parameter value to zero. In the following, Ahmadi et al. [8] studied a new method such as novel control law by compensating flexibility to form a rigid robot. At the same time, an application of the controlled lagrangian method is showed to control an under actuated flexible link in condition of theoretical and experimental conditions [9]. In the recent years, new method such as Unscented Kalman Filter (UKF) has significant role in estimation of the variables state in condition of uncertainties for under-actuated dynamic systems [10]. In this regards, feedback linearization is a common approach used for controlling the nonlinear systems. The approach involves a transformation of the nonlinear system into an equivalent linear system through a change in variables and a suitable control input. Feedback linearization and linear stabilization control of flexible robot was first studied in three-link PUMA [11]. In that case, feedback linearization control of a single link manipulator also was studied for joint elasticity [12]. Similarly, feedback linearization of high speed tracking was applied by model uncertainty for a realistic three-axis robot model [13]. Moreover, Alizadeh et al. [14] focused on the effects of closed-control on the calculation of the Dynamic Load Carrying Capacity (DLCC) for 6R manipulator based on feedback linearization control approach similarily, although all nonlinear dynamics were not removed .Later, feedback linearizing controller was applied for a flexible single-link under gravity and joint friction [15-17]. Regarding the limitation of feedback linearization to remove all nonlinear dynamics and robustness in confronting the uncertainties, the sliding mode has attracted the attention of researchers due to its characteristics of finite time convergence and robustness against uncertainties. Sliding mode control is recognized as a robust control. It is based on the fact that it is much easier to control a first-order system than a general nth-order system. Initially, many studies have been done to improve the sliding mode technique in confronting under-actuated systems such as flexible link robot [18]. In recent decades, robust control by using sliding mode techniques and nonlinear H infinity control design methods is more utilized for flexible-link manipulator [19]. Also, Piltan et al. [20] have done some review on the impact of sliding mode controller on manipulators stability and its application to the robot manipulator in order to design a high performance nonlinear controller in the presence of uncertainties. However, sliding mode lonely could not guarantee robustness in confronting uncertainity. Therefore, a robust control scheme for flexible link robotic manipulators is used based on considering the flexible mechanical structure as a system with slow (rigid) and fast (flexible) modes that can be controlled separately [21]. A new design approach that combines the feedback linearization method, improved SMC compared with other methods for a ball and wheel system [22]. In the following, Calculating the Dynamic Load Carrying Capacity (DLCC) of a spatial cable robot while tracking a desired trajectory based on SMC algorithm could not show the SMC capability [23]. For this reason, a robust chattering-free sliding mode control was proposed in contact-mode for controlling the AFM tip during nano-manipulation process for accomplishment of a precise and effective nano-manipulation task [24]. On the contrary, Yang et al. [25] studied a modified sliding mode in the name of Terminal Sliding Mode Control (TSMC) for two-link flexible manipulators with Non-collocated feedback. Korayem et al. [26] again designed a novel sliding mode controller to compensate the uncertainties of a cable robot and improve its tracking performance. Similar strategy was proposed for the Active Disturbance Rejection Control (ADRC) of a general uncertain system with unknown bounded disturbance based on extended with state observer [27]. Besides, Peza-solis et al. [28] worked on trajectory tracking control in a single flexible-link robot using finite differences and sliding mode. finite

differences is a mathematical expression form but finite difference is a simple algebraic method which was not a powerful combination with the sliding mode in confronting uncertainties. In consequence, an Adaptive Sliding Mode Controller (ASMC) is integrated to design the attitude control for the inner loops of nonlinear coupling dynamic of Unmanned Aerial Vehicle (UAV), Two link flexible manipulator and rollover avoidance in Sport Utility Vehicles (SUV) based on the presents of parametric uncertainities [29-31]. Since the structure of the sliding mode controller requires improvement in adaption with time-varying uncertainties, the researchers are interested in more innovative estimation methods in confronting with time-varying parameter. The neural network, due to educational ability; establishes a proper connection between input and output variables. Fuzzy Adaptive Inference is a powerful tool for predicting results by using available input data, which is a combination of fuzzy inference and artificial neural network. Application of fuzzy sliding mode control applied for robotic manipulator by using multiobjective genetic algorithm seems to be effective in optimizing the parameters [32]. Later, a robust stable fuzzy control via fuzzy modeling and feedback linearization was studied with its applications for controlling uncertain single link flexible joint manipulators [33]. Ahmad et al. [34] worked on the development of composite fuzzy logic control for trajectory tracking and vibration control of a flexible joint manipulator. Consequently, Naderi et al. [35] proposed an optimal reconfiguration strategy of the improved SRR reconfigurable mobile robot based on genetic algorithm and neural network system. Interestingly, control of the flexible joint manipulator via reduced rule-based fuzzy control with experimental validation attracted the attention of researchers [36]. In this regard, Ashraf Ahmad et al. [37] presented the composite fuzzy logic control approach for a flexible joint manipulator similarly. Anyway, hybrid ANFIS–PSO approaches for predicting optimum parameters of a protective spur dike provide remarkable results [38]. And finally, the development of single input fuzzy logic controller for tip angular position tracking and deflection angle reduction of a flexible joint manipulator and optimal robust design of sliding mode control based on multi-objective particle swarm optimization for chaotic uncertain problems offered an interesting combination for controlling flexible links, but it still seemed inevitable to have a proper mathematical relationship in updating the control parameters [39-40].

In the previous literatures, the limitations of feedback linearization in the complete elimination of nonlinear dynamics as well as the sliding mode control structural defects in confronting time-varying uncertainties and fuzzy logic, which did not present a based-model in combination with other controllers were discussed separately. In the present paper, an online hybrid adaptive robust controller is introduced for trajectory tracking of the link angular position and the vibration control of a double flexible joint robot. For this purpose, two novel strategies were proposed based on implementation of an improved hybrid adaptive robust controller and also accurate estimation of control parameters mechanism by using intelligent methods in confronting time-varying uncertainties. In this case, the nonlinear equation is transformed into linear types using feedback linearization in section 3 and then the sliding mode control was applied based on adaptive mechanism to update the controller parameters according to the gradient descent method and the chain rule of differentiation in section 4,5. Finally, multi-objective optimization was used to extract the optimal control parameters. After forming control structure, three intelligent methods: weighting function in section 6.1, adaptive neural network function fitting (ANNF) in section 6.2, and adaptive neuro-fuzzy inference system based on particle swarm optimization (ANFIS-PSO) are used for training an estimator function and approximating the controller parameters in adaption with different values of system's uncertainties in section 6.3. Consequently, in section 7, to prove the robustness of the designed controller in confronting time-varying changes of physical parameters of the robot link and external disturbances, the results are compared with the condition that the values of control parameters are constant and training was not considered. The analysis demonstrated the ability of the trained proposed controller in terms of stability, minimum tracking error and optimal control input.

2 MODEL OF DOUBLE FLEXIBLE JOINT MANIPULATOR ROBOT

The DFJM consists of a rigid link, which is connected to the two extension springs anchored to the solid frame. The driver is a DC servo motor (See "Fig. 1"). When the link is displaced by the force of motor as much as θ , the flexibility of the joints causes the oscillation of the link as the angle of the deflection α as illustrated in the "Fig. 2". The DFJM is a nonlinear and under-actuated system ("Table 1").

The system degree of freedom (DOF) is two in order to link displacement with respect to the fixed system coordination base and angular deflection of link in case of flexible joint. θ in "Fig. 2" denotes the angular displacement and α denotes the angular deflection of the link, therefore the system has two degree of freedom (θ , α) and control input τ which is motor torque.

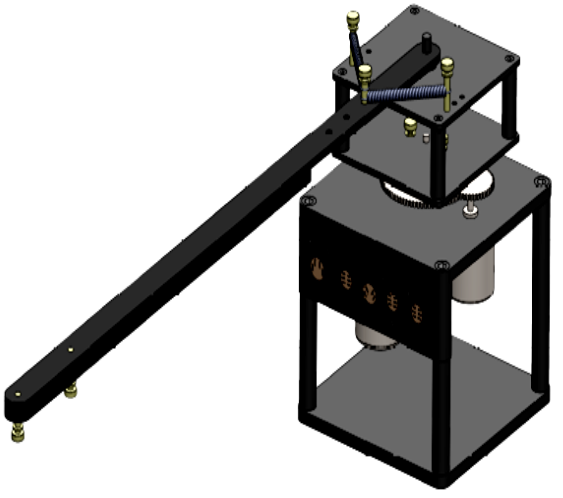

Fig. 1 The double flexible joint manipulator robot system.

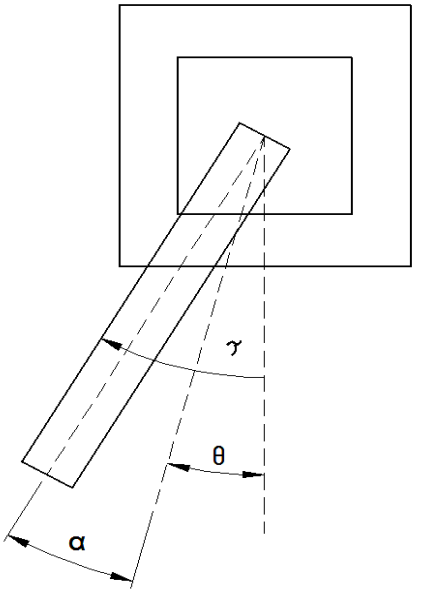

Fig. 2 Parameters in the mathematical model of the double flexible joint manipulator system.

The total kinetic and potential energy (T, V) of the DFJM system is derived as "Eqs. (1) and (2)":

$$T = \frac{1}{2}J_{eq}\dot{\theta}^2 + \frac{1}{2}J_l\left(\dot{\theta}+\dot{\alpha}\right)^2 \tag{1}$$

$$V = \frac{1}{2}K_s\alpha^2 - mghcos(\theta+\alpha) \tag{2}$$

Where, L is:

$$L = T - V$$

Table 1 Physical parameters of the DFJM system [36]

Parameter	symbol	value
Mass of link (Kg)	m	0.403
Gearbox efficiency	η_g	0.9
Motor efficiency	η_m	0.69
Armature resistance (Ω)	R_m	2.6
Total high-gear ratio	K_g	70
Motor torque constant $(\mathrm{N.m/A})$	K_t	7.67×10^{-3}
Motor Back -EMF constant $(\mathrm{V.s/rad})$	K_m	7.67×10^{-3}
Inertial mass of link $\left(\mathrm{Kg.m^2}\right)$	J_l	0.0035
joint stiffness	K_s	1.2485
Equivalent viscous damping coefficient $(\mathrm{N.m.s/rad})$	B_{eq}	0.004
Height of the center of mass (m)	h	0.06
Equivalent moment of inertia $\left(\mathrm{Kg.m^2}\right)$	J_{eq}	0.0026
Gravitational acceleration $\left(\mathrm{m/sec^2}\right)$	g	-9.81

Also $\dot{\theta}$ is the angular velocity of the link and $\dot{\alpha}$ is the angular velocity of the link deflection. The form of Euler-Lagrangian equations are expressed as "Eqs. (3) and (4)":

$$\frac{\partial}{\partial t}\left(\frac{\partial L}{\partial \dot{\theta}}\right) - \frac{\partial L}{\partial \theta} = \tau - B_{eq}\dot{\theta} \tag{3}$$

$$\frac{\partial}{\partial t}\left(\frac{\partial L}{\partial \dot{\alpha}}\right) - \frac{\partial L}{\partial \alpha} = 0 \tag{4}$$

In the following, the dynamic equation of motion from "Eqs. (1–4)" is obtained and briefly displayed in the "Eqs. (5) and (6)":

$$J_{eq}\ddot{\theta} + J_l\left(\ddot{\theta}+\ddot{\alpha}\right) - mghsin(\theta+\alpha) = \tau - B_{eq}\dot{\theta} \tag{5}$$

$$J_l\left(\ddot{\theta}+\ddot{\alpha}\right) + K_s\alpha + mghcos\left(\theta+\alpha\right) = 0 \tag{6}$$

Where, τ is the motor torque determined as "Eq. (7)":

$$\tau = \frac{\eta_m\eta_g K_g K_t\left(V_a - k_m K_g\dot{\theta}_l\right)}{R_m} \tag{7}$$

The symbols in "Eqs. (1–7)" are illustrated in "Table 1". The dynamic behavior of the double flexible joint manipulator system is shown in "Fig. 2" and can be expressed by the following nonlinear "Eqs. (8) and (9)":

$$\dot{x} = f(x) + G.u \tag{8}$$

Where,

$$f(x) = \begin{bmatrix} x_3 \\ x_4 \\ \frac{K_s}{J_{eq}} x_2 - N_2 x_3 \\ N_1 x_2 + N_2 x_3 + \frac{mgh}{J_l} \sin\left(x_1 + x_2\right) \end{bmatrix}, \; G = \begin{bmatrix} 0 \\ 0 \\ N_3 \\ -N_3 \end{bmatrix}. \tag{9}$$

And N_1, N_2, N_3 coefficients of x_2, x_3 are shown in "Eqs. (10-12)":

$$N_1 = \frac{-K_S\left(J_{eq} + J_l\right)}{J_{eq} J_l} \tag{10}$$

$$N_2 = \frac{\eta_m \eta_g K_t K_m K_g^2 + B_{eq} R_m}{R_m J_{eq}} \tag{11}$$

$$N_3 = \frac{\eta_m \eta_g K_g K_t}{R_m J_{eq}} \tag{12}$$

Where the states of "Eqs.(8) and (9)" are defined as $\begin{bmatrix} x_1 & x_2 & x_3 & x_4 \end{bmatrix}^T = \begin{bmatrix} \theta & \alpha & \dot{\theta} & \dot{\alpha} \end{bmatrix}^T$.

3 IMPLEMNETATION OF FEEDBACK LINEARIZATION

A nonlinear control system single input, single output can be consider as "Eqs. (13) and (14)":

$$\dot{x} = f(x) + G(x)u \tag{13}$$

$$y = h(x) \tag{14}$$

Where, $f, G : R \in R^n$ and $x \in R^n$ are the state vectors, $u \in R$ is the vector of inputs and $y \in R^n$ is the vector of output.

The Lie derivative indicates directional derivative of h along the direction of the vector f and repeated Lie derivatives are described as "Eqs. (15-17)":

$$L_f h(x) = \frac{\partial h}{\partial x} f(x) \tag{15}$$

$$L_f{}^2 h(x) = \frac{\partial\left(L_f h(x)\right)}{\partial x} f(x) \tag{16}$$

$$L_f^i h(x) = L_f\left(L_f^{i-1} h\right) = \nabla\left(L_f^{i-1} h\right) f, \; i = 1, 2, 3, \ldots \tag{17}$$

Also, $G(x)$ is the other vector field therefore the scalar function $L_G L_f h(x)$ is determined as"Eq. (18)":

$$L_G L_f h(x) = \left[\frac{\partial\left(L_f h(x)\right)}{\partial x}\right] G(x) = \nabla\left(L_f h(x)\right) G \tag{18}$$

The Lie bracket of $f \in R^n$ and $G \in R^n$ are third vectors field that are defined as "Eq. (19)":

$$ad_f G = [f, G] = \frac{\partial g}{\partial x} f(x) - \frac{\partial f}{\partial x} G(x) = \nabla G f - \nabla f G \tag{19}$$

While, repeated equations of Lie bracket are written as "Eqs. (20) and (21)":

$$ad_f^0 G = G \tag{20}$$

$$ad_f^i G = \left[f, ad_f^{i-1} G\right], i = 1, 2, 3 \ldots \tag{21}$$

When the related degree r of the system is known, if we use the symbols of differential geometry, the derivative of the ith- order shows the output as "Eq. (22)":

$$y^{(i)} = L_f^i h(x) + L_G L_f^{\,i-1} h(x) u = v \tag{22}$$

To design the controller through linearization of all equations, it first needs to be examined whether the system is full-sate-feedback linearizable or not. There is a complete set of states, if and only if, two conditions are the same:

1- The $\mathrm{H}(x) = \left[G(x), ad_f G(x), ad_f^2 G(x), ad_f^3 G(x)\right]$ matrix has a full rank and controllable.

2- The distribution $\Delta = span\left[\mathrm{G}(x), ad_f G(x), ad_f^2 G(x)\right]$ is involutive based on the existing theory and from "Eqs. (15–22)", and computing $det\left(H(x)\right) \neq 0$ system would have a full rank for all the quantities of x_1 and also Δ distribution is involutive.

As a result, there exists an output function $h(x)$ that satisfies the partial differential "Eqs. (23–26)". These

equations are equivalent to a system with a relative degree of 4.
However, by considering the "Eq. (9)", we have the following set of equations:

$$L_G h(x) = 0 \tag{23}$$

$$L_G L_f h(x) = 0 \tag{24}$$

$$L_G L_f^2 h(x) = 0 \tag{25}$$

$$L_G L_f^3 h(x) \neq 0 \tag{26}$$

The answer to the above differential are "Eqs. (27–30)" written as below:

$$h(x) = z_1 = x_1 + x_2 \tag{27}$$

$$L_f h(x) = z_2 = x_3 + x_4 \tag{28}$$

$$L_f^2 h(x) = z_3 = B - \frac{K_s}{J_l} x_2 \tag{29}$$

$$L_f^3 h(x) = z_4 = A(x_3 + x_4) - \frac{K_s}{J_l} x_4 \tag{30}$$

By considering the A and B in "Eqs. (31) and (32)" to reduce the volume of equations "Eqs. (8) and (9)", we have:

$$A = \frac{mgh}{J_l} cos(x_1 + x_2) \tag{31}$$

$$B = \frac{mgh}{J_l} sin(x_1 + x_2) \tag{32}$$

Where, $L_f^4 h(x)$ and $L_G L_f^3 h(x)$ can be obtained as "Eqs. (33) and (34)":

$$\alpha(x) = L_f^4 h(x) = \left(A \frac{K_S}{j_{eq}} + \left(A - \frac{K_S}{j_l}\right) N_1\right) x_2 - \left(\frac{K_S}{j_l}\right) N_2 x_3 + B\left(A - \frac{K_S}{j_l} - (x_3 + x_4)^2\right), \tag{33}$$

$$\beta(x) = L_G L_f^3 h(x) = \frac{K_S}{J_l} N_3 \tag{34}$$

In the following, from "Eq. (22)", the control signal u is defined as "Eq. (35)":

$$u = \frac{1}{L_G L_f^3 h(x)} \left[v - L_f^4 h(x)\right] \tag{35}$$

The state space representation of transformation system is:

$$\begin{bmatrix} \dot{z}_1 \\ \dot{z}_2 \\ \dot{z}_3 \\ \dot{z}_4 \end{bmatrix} = \begin{bmatrix} z_2 \\ z_3 \\ z_4 \\ \alpha(x) + \beta(x) u \end{bmatrix}$$

Where, u_{FBL} can be obtained as "Eq. (36)":

$$u_{FBL} = \left(\frac{K_s}{J_l} N_3\right)^{-1} \left(v - B(x_3 + x_4)^2 - (A \times B) - \left(A \frac{K_s}{j_{eq}} + \left(\left(A - \frac{K_s}{J_l}\right) N_1\right)\right) x_2 + \left(\frac{K_s}{J_l}(B + N_2 x_3)\right)\right) \tag{36}$$

For stabilization, the new control variable v introduced in "Eq. (35)" and appearing in "Eq. (22)", is taken as a linear feedback control as "Eq. (37)":

$$v = -(k_1 z_1 + k_2 z_2 + k_3 z_3 + k_4 z_4) \tag{37}$$

Where, the linear parameters of $[k_1, k_2, k_3, k_4]$ from "Eq. (37)" are obtained from multi-objective Non-Dominate Sorting Genetic Algorithm (NSGA-II) method.
Nevertheless, by using feedback linearization method and elimination of nonlinear terms, could not robust system against uncertainties therefore adaptive sliding mode law technique is utilized to stabilize the flexible joint robotic manipulator.

4 ADAPTIVE ROBUST SLIDING MODE CONTROL

A sliding model controller is a nonlinear controller that can control the system in the presence of structural and non-structural uncertainties. This type of controller, by means of a high-speed switching control rule, between the two control structures, will put the system state variables at a specified level; it will be named the sliding surface. The sliding surface is defined in such a way that always achieves the desired control objectives by pushing the system states towards it. The first part pushes the system to the sliding surface, and the other part is responsible for keeping the states on the sliding surface. In electromechanical systems, the control input u is electrical voltage rather than mechanical and

accelerator forces. Therefore, chattering control of this system in proper frequency range and presence of unmolded dynamics led to design an appropriate switching control law. In this case, to eliminate the chattering, two strategies based on linear interpolation across the boundary layer and tuning the SMC parameters according to the gradient descent method and the chain rule of differentiation were considered.
The sliding surface $\sigma(x,t)$ is defined in "Eq. (38)" and the state-space R^n by the scalar equation, as follows:

$$\sigma(x,t)=\left(\frac{d}{dt}+\lambda\right)^{n-1} e=0\ , \tag{38}$$

Where, λ is a positive constant and it can be explained as the slope of the sliding surface. Since, our system is a four order $x\in R^4$ yielded the "Eq.(39)":

$$\sigma(x,t)=\left(\frac{d}{dt}+\lambda\right)^{3} e=e^{(3)}+3\lambda e^{(2)}+3\lambda^2 e^{(1)}+\lambda^3 e \tag{39}$$

The tracking error defined as $e(t)=y(t)-y_d(t)$ and by considering $y_d(t)=0$ the error function is $e(t)=y(t)$. Differentiating of "Eq. (39)" is given as "Eq. (40):

$$\dot{\sigma}=e^{(4)}+3\lambda e^{(3)}+3\lambda^2 e^{(2)}+\lambda^3 e^{(1)}=y^{(4)}+3\lambda y^{(3)} +3\lambda^2 y^{(2)}+\lambda^3 y^{(1)} \tag{40}$$

As we know from "Eq. (22)" and "Eq. (40)" the $y^{(4)}$ is v Therefore, $\dot{\sigma}$ is as "Eq. (41)":

$$\dot{\sigma}=\alpha(x)+\beta(x)u+3\lambda y^{(3)}+3\lambda^2 y^{(2)}+\lambda^3 y^{(1)} \tag{41}$$

By substituting z_i in the "Eq. (41)", we obtained the "Eq. (42)" as follows:

$$\dot{\sigma}=\alpha(x)+\beta(x)u+3\lambda z_4+3\lambda^2 z_3+\lambda^3 z_2 =a(x)+b(x)u \tag{42}$$

Where, $a(x)$ and $b(x)$ are illustrated as "Eqs. (43) and (44)":

$$a(x)=\alpha(x)+3\lambda z_4+3\lambda^2 z_3+\lambda^3 z_2 \tag{43}$$

$$b(x)=\beta(x) \tag{44}$$

Finally, $a(x)$ and $b(x)$ are determined as "Eqs. (45) and (46)":

$$a(x)=3\lambda\left(A(x_3+x_4)-\frac{K_s}{J_l}x_4\right)+3\lambda^2\left(B-\frac{K_s}{J_l}x_2\right) +\lambda^3(x_3+x_4)+\alpha(x) \tag{45}$$

$$b(x)=\beta(x)=\frac{K_s}{J_l}N_3 \tag{46}$$

For keeping the system states on the sliding surface, the "Eq. (42)" should be equal to zero. Therefore, the equivalent control energy is extracted as "Eq.(47)" :

$$u_{eq}=-\frac{a(x)}{b(x)} \tag{47}$$

Now, to allow the controller resists against disturbances, a discontinuous component is added, and the new controller will be obtained as "Eq. (48)":

$$u_\sigma=u_{eq}+K.sgn(\sigma) \tag{48}$$

Where, K represents the design parameter and $sgn(\sigma)$ is the sign of switching near the sliding surface. For reducing the chattering, $sgn(\sigma)$ is replaced with saturation function and defined as "Eq. (49)":

$$u_\sigma=u_{eq}+K.sat\left(\frac{\sigma}{\varphi}\right) \tag{49}$$

Therefore,
u_σ is determined as "Eq. (50)":

$$u_\sigma=-\left(\frac{K_s}{J_l}N_3\right)^{-1}\left((\alpha(x))+\left(3\lambda\left(A(x_3+x_4)-\frac{K_s}{J_1}x_4\right)\right)\right. \left.+\left(3\lambda^2\left(B-\frac{K_s}{J_1}x_2\right)\right)+\left(\left(\lambda^3(x_3+x_4)\right)\right)+\left(Ksat\left(\frac{\sigma}{\varphi}\right)\right)\right) \tag{50}$$

The saturation function in "Eq. (49)" is defined as"Eq. (51)":

$$sat\left(\frac{\sigma}{\varphi}\right)=\begin{Bmatrix} -1 & : & \frac{\sigma}{\varphi}<-1 \\ \frac{s}{\varphi} & : & -1<\frac{\sigma}{\varphi}<1 \\ 1 & : & \frac{\sigma}{\varphi}>1 \end{Bmatrix} \tag{51}$$

Where, the φ is the thickness of the boundary layer. The boundary φ limited the motion of system as it slide along the definite surface $\sigma(x,t)$.

5 PROPOSED CONTROLLER

The proposed controller has both adaptive and robust features, simultaneously. In fact, by using feedback linearization method, the nonlinear dynamics were removed. Then SMC was applied because this controller is robust in confronting uncertainties and is suitable for nonlinear control dynamic systems. But since the structure of the SMC required some changes to make more appropriate performance in confronting uncertainties, two strategies based on linear interpolation across the boundary layer and tuning the SMC parameters according to the gradient descent method and the chain rule of differentiation were considered. In the following, to implement adaptation law and update two parameters (K,φ) of sliding mode controller and considering the Lyapunov stability theory, we have "Eqs. (52) and (53)":

$$V = \frac{\sigma^2}{2} \tag{52}$$

$$\dot{V} = \sigma\dot{\sigma} < 0 \tag{53}$$

By substituting "Eqs. (38–50)" with "Eq. (42)" and multiplying both sides of the obtained equation into σ , "Eq. (54)" is obtained as follows:

$$\sigma\dot{\sigma} = \left(z_4 + 3\lambda z_3 + 3\lambda^2 z_2 + \lambda^3 z_1\right)\left(a(x) + b(x)u\right) \tag{54}$$

Thus, when $t \to \infty$ then $\sigma(t) \to 0$. A gradient search method is utilized to minimize the sliding condition $\sigma\dot{\sigma}$ and obtain an adequate adaptation mechanism for time-varying two parameters of SMC by deriving through the chain rule of differentiation according to "Eqs. (55) and (56)":

$$\dot{K} = -\gamma_1 \frac{\delta(\sigma\dot{\sigma})}{\delta K} = -\gamma_1 \frac{\delta(\sigma\dot{\sigma})}{\delta u_\sigma}\frac{\delta u_\sigma}{\delta K} \tag{55}$$

$$\dot{\varphi} = -\gamma_2 \frac{\delta(\sigma\dot{\sigma})}{\delta \varphi} = -\gamma_2 \frac{\delta(\sigma\dot{\sigma})}{\delta u_\sigma}\frac{\delta u_\sigma}{\delta \varphi} \tag{56}$$

By computing $\frac{\delta(\sigma\dot{\sigma})}{\delta u_\sigma}$, $\frac{\delta u_\sigma}{\delta K}$ and $\frac{\delta u_\sigma}{\delta \varphi}$ we have:

$$\frac{\delta(\sigma\dot{\sigma})}{\delta u_\sigma} = \sigma.b(x) \tag{57}$$

$$\frac{\delta u_\sigma}{\delta K} = sat\left(\frac{\sigma}{\varphi}\right) \tag{58}$$

$$\frac{\delta u_\sigma}{\delta \varphi} = K\, d/dt\left(sat\left(\frac{\sigma}{\varphi}\right)\right).\left(-\frac{\sigma}{\varphi^2}\right) \tag{59}$$

Finally, $\dot{K}$ and $\dot{\varphi}$ from "Eqs. (57–59) " are derived as "Eqs. (60) and (61)":

$$\dot{K} = -\gamma_1 \sigma b(x) sat\left(\frac{\sigma}{\varphi}\right) \tag{60}$$

$$\dot{\varphi} = \gamma_2 K b(x)\, d/dt\left(sat\left(\frac{\sigma}{\varphi}\right)\right).\left(\frac{\sigma}{\varphi}\right)^2 \tag{61}$$

Where, $\dot{K}$ and $\dot{\varphi}$ are determined as "Eqs. (62) and (63)":

$$\dot{K} = -3\lambda\gamma_1\left(A\left(x_3 + x_4\right) - \frac{K_s}{J_l}x_4\right)\left(\frac{K_s}{J_l}N_3\right)sat\left(\frac{\sigma}{\varphi}\right) - 3\lambda^2\gamma_1\left(B - \frac{K_s}{J_l}x_2\right)\left(\frac{K_s}{J_l}N_3\right)sat\left(\frac{\sigma}{\varphi}\right) - \lambda^3\gamma_1\left(x_3 + x_4\right)\left(\frac{K_s}{J_l}N_3\right)sat\left(\frac{\sigma}{\varphi}\right) \tag{62}$$

$$\dot{\varphi} = \gamma_2 K\left(\frac{K_s}{J_l}N_3\right) d/dt\left(sat\left(\frac{\sigma}{\varphi}\right)\right).\left(\frac{\sigma}{\varphi}\right)^2 \tag{63}$$

Finally, γ_1 and γ_2 are learning rate and positive and $d/dt\left(sat\left(\frac{\sigma}{\varphi}\right)\right)$ is defined as "Eq. (64)".

$$d/dt\left(sat\left(\frac{\sigma}{\varphi}\right)\right) = \begin{cases} 0 & : \quad \frac{\sigma}{\varphi} < -1 \\ 1 & : \quad -1 < \frac{\sigma}{\varphi} < 1 \\ 0 & : \quad \frac{\sigma}{\varphi} > 1 \end{cases} \tag{64}$$

By updating two parameters of K and φ , the main architecture of the control approach utilized in the present study is based on the proposed control method which yields as "Eq. (65)":

$$u = u_{FBL} + u_{ARSMC} \tag{65}$$

Where, u_{FBL} is the FBL techique effort and u_{ARSMC} stands for the adaptive robust sliding mode control effort. The block diagram of the proposed controller is displayed in "Fig. 3".

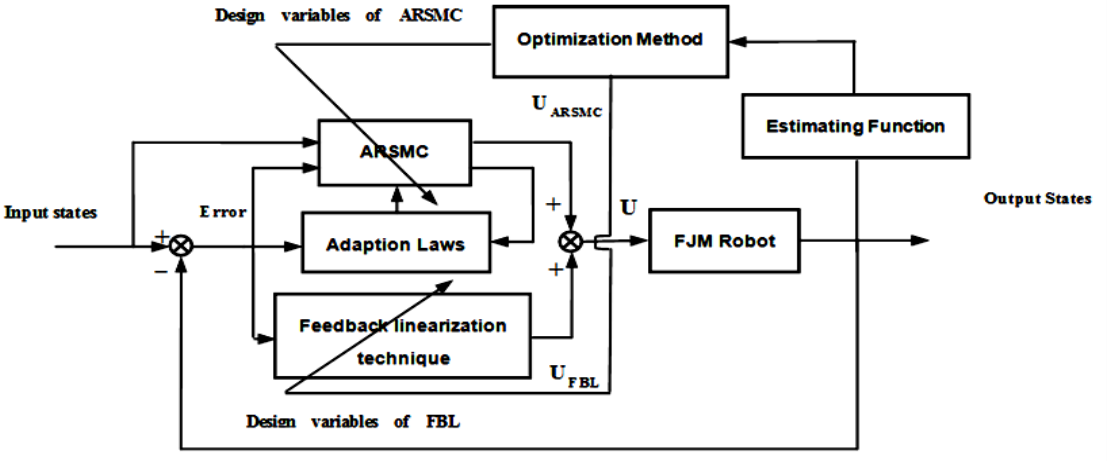

Fig. 3 Block diagram of the proposed controller for the double flexible joint manipulator robot system.

6 ESTIMATION FUNCTION MECHANISM

Based on the three proposed methods, the estimator function trains the values of the optimal control parameters and updates these values simultaneously with time-varying change of the link physical parameters.

6.1. Weighting Function Estimator

In this method, as mentioned previously, the uniform distribution of 60 samples of optimal control coefficients, proportional to the changes in mass and length of the link is generated by a hybrid single objective algorithm GA-PSO which is named y_{ctual} .The sixthy samples distribution of designed parameters is demonstrated in "Figs. 4-6".

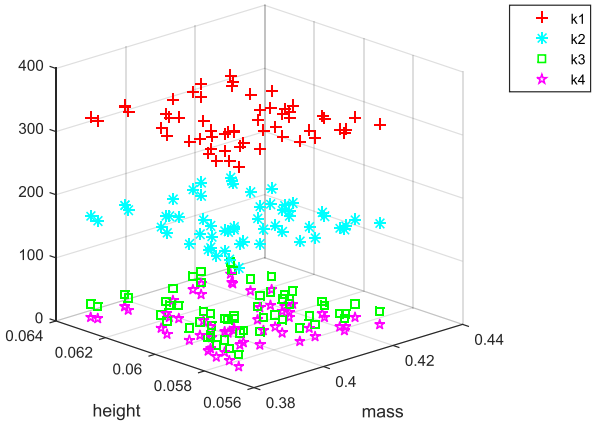

Fig. 4 Distribution of k_1, k_2, k_3 and k_4 by GA-PSO.

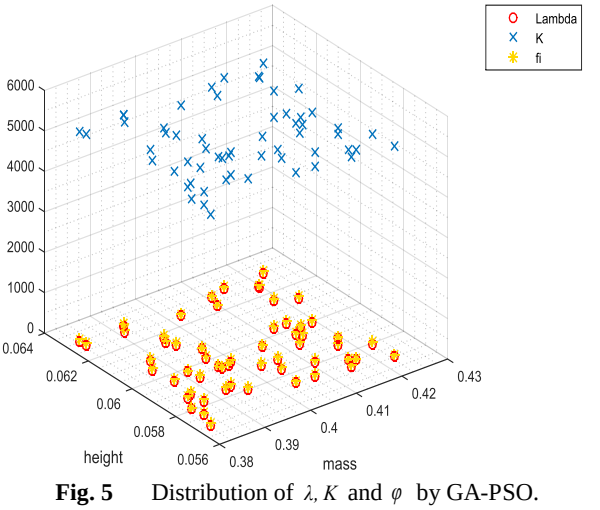

Fig. 5 Distribution of λ, K and φ by GA-PSO.

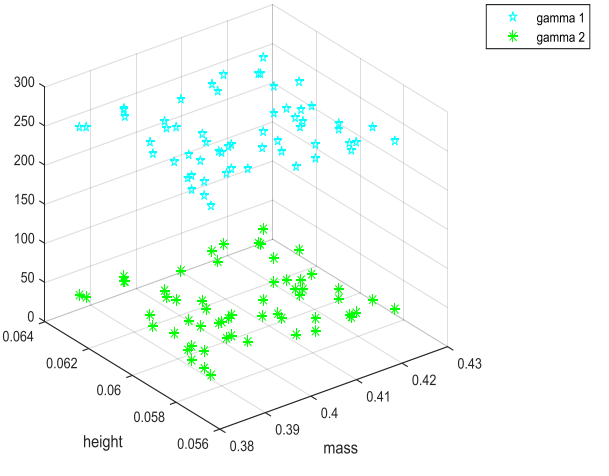

Fig. 6 Distribution of γ_1, γ_2 by GA-PSO.

In the following, for each control coefficients, a relation is determined according to the variable parameters with time or as the estimator function, considered as "Eq. (66)".

$$y_{estimated\ i} = f\left(X_i, w\right) \tag{66}$$

In which, x_i the vector of variable parameters varied with time, w is the vector of weight coefficients and the target is determining constant coefficients w_j in such a way that minimizes the Root Square Mean Error that can be expressed in the "Eq. (67)".

$$RSME = \sqrt{\frac{\sum_{i=1}^{n}\left(y_{actual\ i} - y_{estimated\ i}\right)}{n}} \tag{67}$$

Where, n is the number of samples which is 60 number and RSME is Root Square Mean Error. In fact, after generating suitable w_j by the GA-PSO algorithm, a relation according to the system parameters for each control coefficients will be obtained that could be estimated at any moment by changing the mass and height of parameters of the system which generates the optimal control coefficients. As a result the control law by using the estimator function always generates optimal control coefficients and provides optimal control law for the system in confronting time-varying uncertainties. The estimator function for all control coefficients is an exponential type and is considered as the "Eq. (68)".

$$y_{estimated} = w_1 + w_2 m^{w_3} + w_4 h^{w_5} \tag{68}$$

The variation of physical parameters is considered as stepping function diagram in which the values changed with time. In the following, when the parameters m and h change with time, the response of the system state variables are used for both cases, and the controller uses an optimal constant value for the control coefficients and another mode in which the estimator functions received the physical parameters (m,h) and update the optimal control coefficients online.

Then, by using a hybrid single objective GA-PSO algorithm and considering the objective function "Eq. (66)" and definition of w_j in "Eq. (68)", each control coefficients get minimized.

6.2. Adaptive Neural Network Function Fitting estimator (ANNF)

Artificial neural network is one of the computational methods that by the process of learning (by using processors named neurons) tries to provide a mapping between the input data (input layer) and the desired space (output layer). The system consists of a large number of highly interconnected processing elements named neurons that work together to solve a problem. Each neural network consists of three layers of input, hidden and output, respectively. There are a number of processors called neurons in each layer. The hidden layers process the information received from the input layer and provide the output layer. The transfer function expresses the response of each neuron to its input signal. Common transmission functions used in artificial neural networks are sigmoid function and hyperbolic tangent. Each network receives training examples. Education is a process that ultimately leads to learning Network. Learning is done when the weights of the communication between layers change so that the difference between the predicted and calculated values is acceptable [41-42]. In this case, the input data to present the network includes physical parameters of the link and output is optimal control coefficients. The trained output data was updated in an online way with input according to Levenberg-Marquardt back propagation algorithm. The function estimator is determined as "Eq. (69)".

$$y_{estimated\ i} = f\left(\sum w_i^T x_i + b\right) \tag{69}$$

In which, x_i is the vector of variable parameters varied with time, and b also is constant and w is the vector of weight coefficients and the target is determining constant coefficients w_j in such a way that tunes the $y_{estimatedi}$ and minimizes the Root Square Mean Error of the "Eq. (67)".

6.3. Adaptive Neuro-Fuzzy Inference System and Particle Swarm Optimization function estimator (ANFIS-PSO)

Neural network, due to their educational ability, can create a proper connection between input and output variables. Fuzzy Adaptive Inference is a powerful tool for predicting results using available input data, which is a combination of fuzzy inference and artificial neural network [43]. A fuzzy neural network, a combination of fuzzy logic and neural network, is a powerful processing tool. Adaptive neural network is a multimedia neural network in which each node has a specific function on the input data as well as a set of parameters related to this node. For each input, there are two fuzzy rules (IF-THEN), the maximum value is 1 and the minimum value is 0, to map it to the output space. ANFIS employs gradient descent algorithm for tuning parameters which defines membership functions. Least squares method is used for consequent parameters that describes the coefficients of each equation by ANFIS to identify them. In this paper, for enhancing the performance of ANFIS instead of hybrid learning method, Particle Swarm Optimization (PSO) algorithm is applied for tuning and

adjusting the parameters of membership function. This method has n inputs and for each input, the membership function is considered as $m_1, m_2, \cdots, m_m$, respectively. So the numbers of rules in this method are $M = m_1 \times m_2 \times \cdots \times m_m$ and the rules for Sugeno method are as follows:

$$RuleK: \ If \ \ x_1 \ is \ A_1^K \ and \ x_2 \ is \ A_2^K \ and \ \cdots x_m \ is \ A_M^K$$
$$then \ \ F^K = a_{K0} + a_{K1}x_1 + \cdots + a_{KN}x_N \qquad K = 1, \cdots, \mathrm{M}$$

Where, a_{KM} is truth value of membership function and x_i vector of input variables. The function estimator is determined as "Eqs.(70) and (71)":

$$y_{estimatedi}(k) = \frac{\sum_{j=1}^{M} F_j \prod_{i=1}^{n} exp\left[- \frac{\left[x_i(k) - m_{ij} \right]^2}{\left(c_{ij} \right)^2} \right]}{\sum_{j=1}^{M} \prod_{i=1}^{n} exp\left[- \frac{\left[x_i(k) - m_{ij} \right]^2}{\left(c_{ij} \right)^2} \right]} \tag{70}$$

$$w_{ij} = exp\left[- \frac{\left[x_i(k) - m_{ij} \right]^2}{\left(c_{ij} \right)^2} \right] \tag{71}$$

Where, w_{ij} in "Eq. (71)" is the vector of weight coefficient, m_{ij} is Gaussian membership function center and c_{ij} is the value of standard deviation. The Root Square Mean Error can be calculated same as the "Eq. (67)".

7 THE RESULTS OF IMPLEMENTATION OF PROPOSED CONTROLLER

In this study, we utilized two innovative methods, including exclusion of chattering by eliminating the discontinuity of the control law based on linear interpolation across the boundary layer and proposing new mathematical relati-onships to update the sliding mode parameters for minim-izing tracking error of angular position and deflection of link. In this step, after forming the control structure; Non-Dominate Sorting Genetic Algorithm (NSGA-II) is used to extract the optimal parameters by considering two objective functions which includes minimizing the error of the link angular position and deflection and also the controller input according to the "Eqs. (72) and (73)":

Due to the limitations of sliding mode controller which was mentioned in the introduction it seems necessary to improve the structure of the proposed controller. So, as mentioned earlier, two innovative strategies based on updating parameters in accordance with proposed mathematical model and linear interpolation method around boundary layer of sliding surface in order to removing chattering and sliding surface were considered. Also to enhance the performance of the proposed controller, reconfiguration with an optimized feedback linearization control with respect to robustness in confronting parametric and non-parametric uncertainties was on our agenda. But such a complex control with multiple parameters requires the proper training of parameters in confronting the parametric and non-parametric uncertainties. Eventually, training an estimator according to three methods was considered for predicting proper design variables in confronting parametric uncertainties and external disturbance. In order to prove the designed control ability, the output state results of three suggested methods are compared (Weighting Function, ANNF and ANFIS-PSO) with ARSM-FBL controller.

The vector $[k_1, \ k_2, \ k_3, \ k_4, \ \gamma_1, \ \gamma_2, \ \lambda, \ K_0, \ \varphi_0]$ is the one for design variables (selective parameters) of the controller. Hence, k_1, k_2, k_3 and k_4 are positive constants; λ, K_0 and φ_0 are the coefficients of sliding surface and γ_1, γ_2 are the learning rates of "Eqs. (60) and (61)" and are positive. Furthermore, the objective functions of this problem are defined as "Eqs. (72) and (73)":

$$f_1 = \int_0^T |e_1(t)| \, dt + \int_0^T |e_2(t)| \, dt \tag{72}$$

$$f_2 = \int_0^T |u(t)| \, dt + max_{t=0}^{T}\left(|u(t)| \right) \tag{73}$$

The $e_1(t) = x_1(t) - y_d(t)$ is the error of link angular position and $e_2 = x_2(t) - y_d(t)$ is the error of link angular deflection. By considering $y_d(t) = 0$, therefore the error function $e_i = x_i(t)$. Moreover, $u(t)$ stands for the control effort from time 0 to T. The value of T is equal to 15 seconds.

The boundary of k_1, k_2, k_3 and k_4 are lies between 0 and 1000; the boundary of γ_1 and γ_2 are lies between 0 and 400 and the boundary of λ is lay between 0 and 10; the initial condition $[\theta \ \ \alpha \ \ \dot{\theta} \ \ \dot{\alpha}]^T$ is defined as $\left[-\frac{\pi}{180} \ \ 0 \ \ 0 \ \ 0 \right]^T$.

The Pareto front in "Fig. 7", is obtained on the basis of strength Pareto evolutionary algorithm (NSGA-II). In the following, "Figs. 8-12" and "Table 2"demonstrated the optimal adaptive robust sliding mode and feedback linearization technique (ARSMC-FBL), respectively. Similarly, points A, B, C and D represent the optimal points of ARSM-FBL and FBL controllers, selected from their respective Pareto fronts. The comparison results of the proposed controller with FBL demonstrated appropriate performances in lower settling time and overshoot.

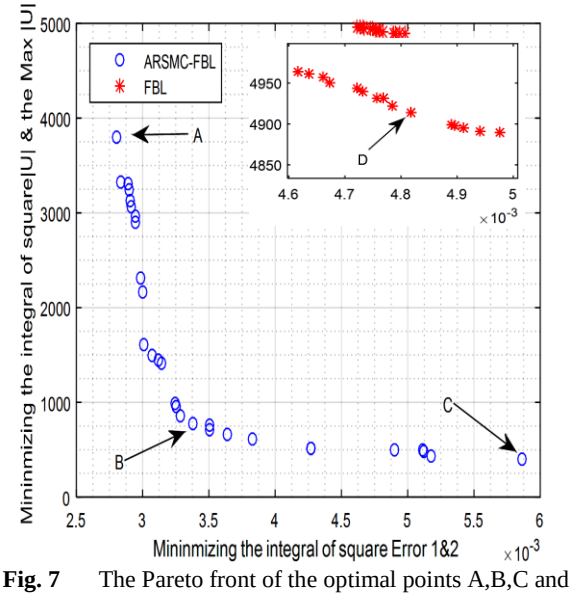

Fig. 7 The Pareto front of the optimal points A,B,C and D for the DFJM system. The Iteration number is 100.

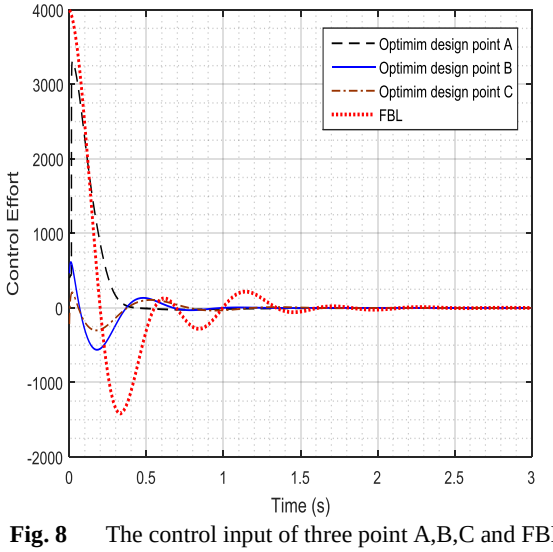

Fig. 8 The control input of three point A,B,C and FBL, shown in pareto front.

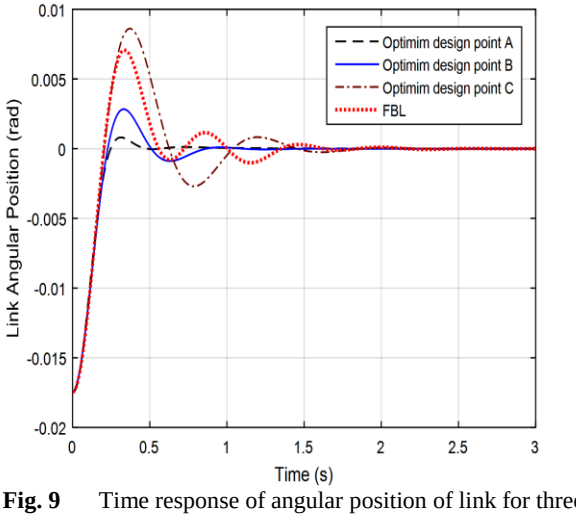

Fig. 9 Time response of angular position of link for three points of A,B,C and FBL, shown in pareto front.

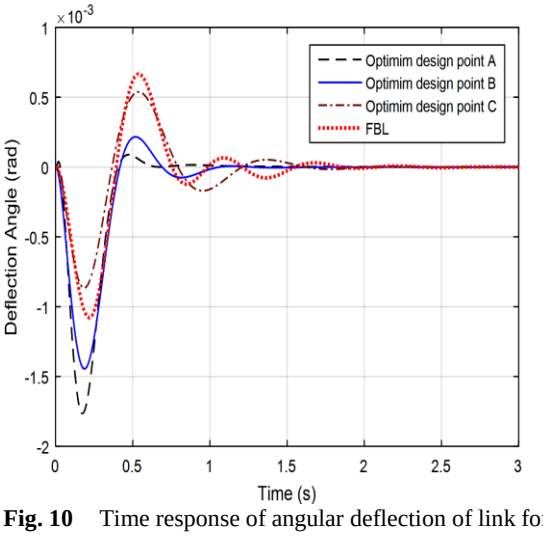

Fig. 10 Time response of angular deflection of link for three points of A,B,C and FBL, shown in pareto front.

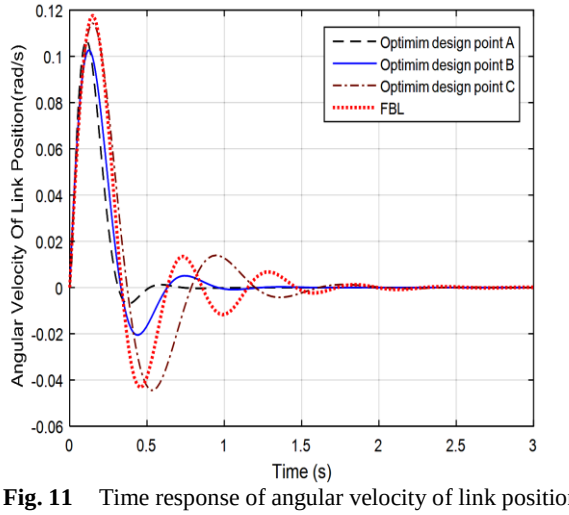

Fig. 11 Time response of angular velocity of link position for three points of A,B,C and FBL, shown in pareto front.

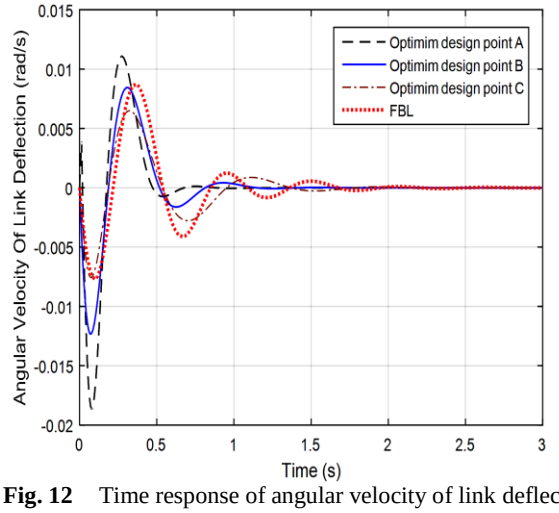

Fig. 12 Time response of angular velocity of link deflection for three points of A,B,C and FBL, shown in pareto front.

In the following, to implement the estimator function we consider ± 5 percentage changes of link physical parameters and simultaneous external disturbance is added. respectively. The mass and height of link tolerance values are determined as follows :

$$m \in [0.38285,\ \ 0.42315]$$

$$h \in [0.057,\ \ 0.063]$$

Assuming the step changes of the mass (m) and the height of link mass center (h), the uniform distribution of these two physical parameters is generated by applying a hybrid algorithm which is combination of genetic algorithm and particle swarm optimization GA-PSO [44]. Eventually, for each physical parameter of link (m, h), 60 samples of optimal control coefficients are produced by GA-PSO algorithm. The objective function is determined as "Eq.(74)".

$$f_3 = \int_0^T |\, e_1(t)\,|\, dt + \int_0^T |\, e_2(t)\,|\, dt + \int_0^T |\, u(t)\,|\, dt + max_{t=0}^{T}\left(|\, u(t)\,|\right) \tag{74}$$

Table 2 Objective functions and their associated design variables for the Optimum points illustrated in Fig. 7

Design variable	Proposed controller			FBL
	Point A	Point B	Point C	Point D
f_1	0.002804	0.005863	0.003378	0.004816
f_2	3802.9924	408.2462	776.6331	4913.5704
k_1	57.5019	315.7167	329.6447	636.8911
k_2	843.9626	558.7352	169.6146	570.1993
k_3	217.6351	34.8271	34.1281	32.1279
k_4	18.7381	13.0941	15.2735	10.5603
λ	1.5563	9.4526	8.3397	---
$K_\circ$	3789.6495	4678.4326	5214.3991	---
$\varphi_\circ$	1.118144	49.6325	60.4122	---
γ_1	146.0856	275.2667	263.6551	---
γ_2	31.9456	42.5641	45.4168	---

In the weighting function method, the w_j values of "Eqs. (66) and (68)" were extracted by single objective genetic algorithm for each optimal control coefficients and are determined in such a way that the RSME of "Eq. (67) " gets minimized.

As mentioned in the ANNF method, in order to estimate the optimal values and to train an estimator function for updating the values of the control coefficients, 10 numbers of hidden neurons are considered for the artificial neural network fitting and the output is the results of estimated values that are adapted with online variation of m and h.

In ANFIS-PSO method, similar to ANNF, to examine the performance of ANFIS-PSO the optimum designed parameters are the inputs of estimator function. At the next step, the FIS model tuning based on Takagi-Sugeno stru-cture will be the outcome of its operation. Tuning means positioning terms in the universe of the input variable and selecting functional parameters for the relati-onship between output and input with reference to an output variable. The superior purpose of tuning is to reach settings of the FIS model parameters that will

make it to represent the relationship between output and input contained in the training data obtained from the dynamic model with minimal error. Finally, "Figs. 13-15" and "Table 3" present the system states variable response in the presence of external disturbance and time-varying physical parameters of the link (m, h) in case of proposed controller using constant values for its parameters (offline), and condition that the estimator function at any moment calculates the control coefficients with respect to the changes of m, h (online). Also "Figs. 16 and 17" demonstrated the φ and K variation in the same conditions.

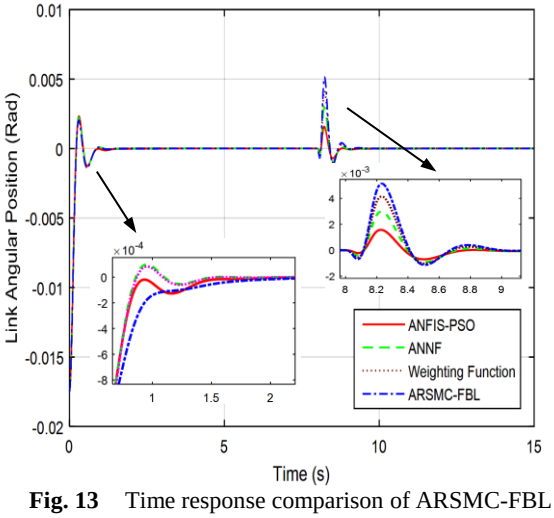

Fig. 13 Time response comparison of ARSMC-FBL angular position of link for optimal design point B with other three methods in condition of parametric and non-parametric uncertainties.

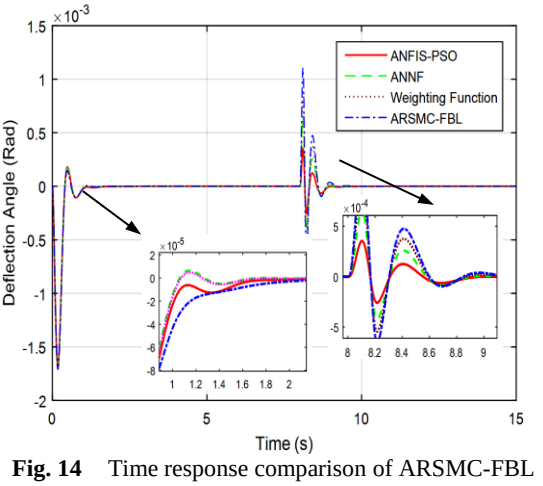

Fig. 14 Time response comparison of ARSMC-FBL angular deflection of link for optimal design point B with other three methods in condition of parametric and non-parametric uncertainties.

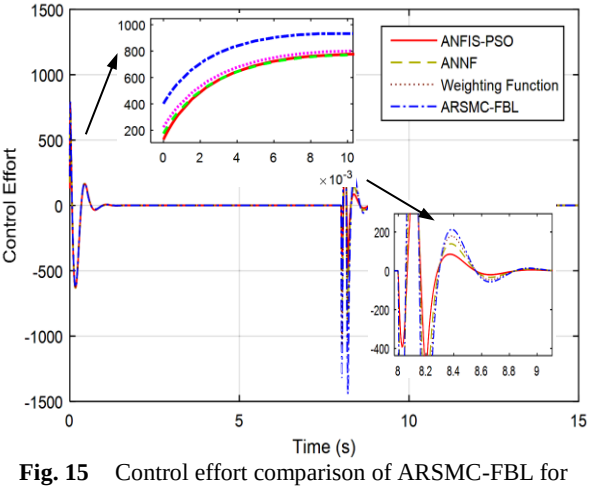

Fig. 15 Control effort comparison of ARSMC-FBL for optimal design point B in condition of parametric and non-parametric uncertainities.

Table 3 The comparison results of the settling time, overshoot of the DFJM system in condition of parametric and non-parametric uncertainities

Method	Without External Disturbance				f_3	With External Disturbance				f_3
	Settling time (seconds)		Over shoot (radian)	Over shoot (radian)		Settling time (seconds)		Over shoot (radian)	Over shoot (radian)	
	Link position	Link deflection	Link position	Link deflection		Link position	Link deflection	Link position	Link deflection	
ANFIS-PSO	1.237	1.143	0.00018	0.0023	949.4	9.406	9.651	0.00156	0.000124	1045.5
ANNF	1.244	1.085	0.00017	0.0022	946.7	9.499	9.696	0.00298	0.000259	1246.9
W.F.	1.270	1.153	0.00014	0.0020	975.0	9.573	9.733	0.00413	0.000374	1598.9
ARSMC-FBL	1.420	1.308	0.00010	0.0016	1050.9	9.843	9.938	0.00512	0.000471	1890.4

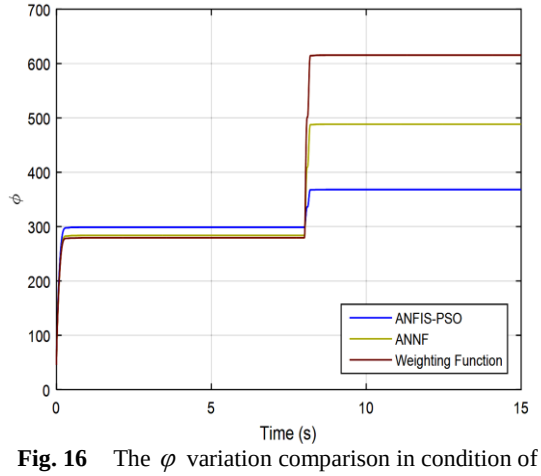

Fig. 16 The φ variation comparison in condition of parametric and non- parametric uncertainities.

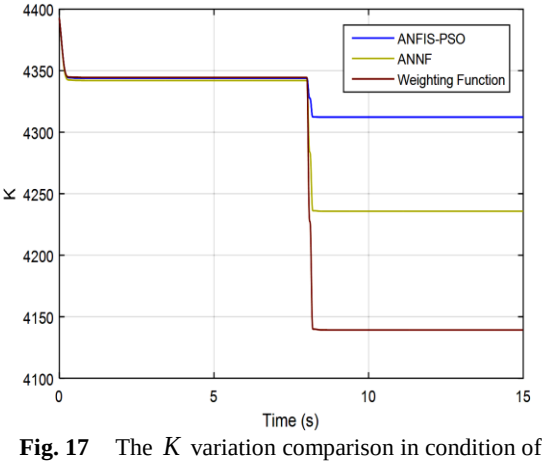

Fig. 17 The K variation comparison in condition of parametric and non-parametric uncertainities.

In "Fig. 7" by considering the majority of points in the Pareto front, the Pareto solution of the ARSMC-FBL is superior to the Pareto solutions of FBL technique. It means that the proposed approach yields a better Pareto front.

In the following, By analyzing the "Figs. 8-12" and "Table 2" it is concluded that the optimal parameters of the pro-posed controller have better tracking error and control input in comparison with FBL. Indeed, the flexible joint man-ipulator system due to simultaneous utilization of two controller's feature achieved stability with minimum tracking error and control effort in the shortest possible time.

To examine the performance of the control system with different initial conditions, after the system converges to the equilibrium, a sinsuidal disturbance is added by pushing the link away from the equilibrium position in the 8th second as "Eq. (75)".

$$\begin{cases} y = \sin\left(\dfrac{(t-8)\times\pi}{0.1}\right)\times 0.7 \\ \text{if} \\ t > 8 \quad \& \quad \& \quad t < 8.2 \end{cases} \tag{75}$$

According to the values given in "Table 3" and "Figs. 13-15", the results of settling time, overshoot of angular position and link deflection for three methods (ANFIS-PSO, ANNF and WF) were displyed. The results demonstrated better performances in comparison with condition that estimation was not considered. Moreover, the values of objective function "Eq. (74)" are shown in "Table 3" which is the sum of link angular position and deflection errors and integral of absolute control input for ARSMC-FBL is greater than other three estimation methods in condition of parametric and non-parametric uncertainties.

According to the results of "Table 3", three methods (ANFIS-PSO, ANNF, WF), which are the time response of the link angular position and deflection of the DFJM, reache to stability of 1.237, 1.244, 1.270 and 1.143, 1.085, 1.153 seconds faster than ARSMC-FBL method in 1.420 and 1.308 seconds, respectively. Also the control effort of three methods 949.41, 946.73 and 975.03 are lower than 1050.98 of ARSMC-FBL value without training procedure, respectively. By analyzing "Figs. 13-15" and "Table 3", it can be concluded that the optimal parameters of the trained proposed controller have better settling time and control input in comparison with ARSMC - FBL controllers in the absence of non-parametric uncertainties. Indeed, the double flexible joint manipulator robot system achieves the stability with less oscillation and energy consumption.

In the following, to verify the robustness of the trained proposed controller in condition of non-parametric uncertainties, the link was pushed suddenly away from the equilibrium position and the disturbance effect on the link was shown according to "Eq. (75)". The results of "Table 3" in condition of disturbance indicate that the angle of link converges to the stability in 9.406, 9.499, 9.573 seconds and the angular deflection of link converges to the stability in 9.651, 9.696, 9.733 seconds, for three methods which is lower than ARSMC-FBL method, 9.843 and 9.938 seconds without training procedure in condition of external disturbance, respectively. Besides, the control input values of the ANFIS-PSO, ANNF, and Weighting Function are 1045.52, 1246.91 and 1598.99 which demonstrates significant reduction in comparison with ARSMC-FBL method. According to these results, the proposed controller exhibits good performance in the presence of parametric and non-parametric, especially in the ways that the estimator function predicts the values of the optimal design variables. The results of RSME for

different methods of ANFIS-PSO, ANNF and Weighting Function are demonstrated in "Table 4". As can be seen, the values of root mean square for the trained proposed controller parameters were minimized, which means that the variance of the actual and estimated parameters is minimal. In "Figs. 16 and 17", the process of updating φ and K is shown in presence of impulsive disturbance for different methods. It demonstrated that in 8th second step changes occurred as soon as the link hit and the parameters adapted to the new condition in order to converge the system into the stability.

Table 4 The results of average RSME values of Eq (67) for three methods of ANFIS-PSO, ANNF, Weighting function estimator

RSME Values of Three Methods	λ	K_o	φ_o	γ_1	γ_2	k_1	k_2	k_3	k_4
ANFIS-PSO	0.03309	3.5757	0.7408	1.009	1.8885	1.6673	1.3705	0.08715	0.00247
ANNF	0.0933	1.5530	0.3276	1.0372	1.9048	1.8787	1.5546	0.1506	0.0013
W.F.	0.0696	5.1214	1.0128	2.7424	1.5641	2.2173	2.3184	0.6063	0.0049

Consequently, the analysis of "Figs. 7-17" and "Table 2, 3 and 4" reveals that the optimized trained controllers demonstrates an appropriate performance in confronting parametric and non-parametric uncertainties and also proves that it has been able to provide robustness and stability in all aspects of settling time, overshoot and control input for the flexible joint manipulator.

8 CONCLUSION

In this paper, a novel online hybrid adaptive robust controller based on non-dominate sorting genetic algorithm (NSGA-II) is presented for a double flexible joint manipulator robot. Since, the DFJM offers various benefits such as flexibility, faster performance, lower weight and power consumption; these features move towards to design a complex controller. The aim of the proposed controller is to reach stability and trajectory tracking of the DFJM link by minimizing the error of angular position and deflection and achieve an optimal control inputs. For this reason, after transforming the nonlinear equation into linear types and applying the adaptive mechanism to update the optimal parameters, the chattering appears on the system. Since the proposed controller structure needs to be improved, adaptive mechanism based on gradient descend method and chain rule of the derivation (a novel mathematical realation) and optimization of the design parameters based on multi-objective evolutionary algorithm were proposed. Moreover, in the second step to evaluate the proposed controller ability in confronting parametric and non-parametric uncertainties training, an estimator function was on the agenda. The target of training an estimator function is to obtain control parameters that could adapt with time-varying changes of the DFJM's link physical parameters.

Finally, the results revealed better error performances and optimal control inputs in comparison with a condition that the controller parameters values are constant and training was not considered. Eventually, the analysis demonstrated the robustness and proper performance of the trained proposed controller in respect of stability, minimum tracking error, overshoot and optimal control efforts in condition of parametric and non-parametric uncertainties.

REFERENCES

[1] Eva, G., Dmitri, S., Tracking Controller for Flexible Joint Robots, Journal of Electrical Engineering, Vol. 53, No. 7-8, 2002, pp. 184-190.

[2] Kolhe, J. P., Shaheed, M. D., Chandar, T. S., and Talole, S. E., Robust Control of Robot Manipulators Based On Uncertainty and Disturbance Estimation, International Journal of Robust And Nonlinear Control, Vol. 23, No. 1, 2013, pp. 104-122.

[3] Marutheswar, G. V., Chandrakala, C., Control of Rotary Flexible Link with Linear Quadratic Regulator, International Journal of Engineering Research and Applications, Vol. 3, No. 1, 2013, pp. 1699-1703.

[4] Mbede, J. B., Mvogo Ahanda, J. J., Exponential Tracking Control Using Backstepping Approach for Voltage-Based Control of a Flexible Joint Electrically Driven Robot, Journal of Robotics, No. 1, 2014, pp. 1-10.

[5] Haouari, F., Nourdine, B., Boucherit, M. S., and Tadjine, M., A Coefficient Diagram Method Controller with Back Stepping Methodology for Robotic Manipulators, Journal of Electrical Engineering, Vol. 66, No. 5, 2015, pp. 270–276.

[6] Liu, Z. G., Huang, J. M., A New Adaptive Tracking Control Approach for Uncertain Flexible Joint Robot System, International Journal of Automation and Computing ,Vol. 12, No. 5, 2015, pp. 559–566.

[7] Qingxuan, J., Xiaodong, Z., Hanxu, S., and Ming, C., Active Control of Space Flexible-Joint/Flexible-Link Manipulator, IEEE Conference on Robotics, Automation and Mechatronics, Beiging, China, 2008, pp. 1-7.

[8] Ahmadi, S., Fateh, M. M., Control of Flexible Joint Robot Manipulators by Compensating Flexibilty, Iranian Journal of Fuzzy Systems, Vol. 15, No. 4, 2018, pp. 57-71.

[9] Ettefagh, M. H., Naraghi M., and Mahzoon, M., Experimental Control of a Flexible Link by the Method of Controlled Lagrangian, Journal of Theoretical and Applied Vibration and Acoustics, Vol. 4, No. 1, 2018, pp. 81-98.

[10] Pezhman, A., Masoumnezhad, M., and Nouraifar, V., Optimize the Motion Model of Overhead Crane with Accurate Estimate the Equation of Variables State by using Unscented Kalman Filter, 3rd International Conference on Research in Science and Technology, Berlin, Germany, 2016, pp. 1-9.

[11] Lih-Chang, L., King, Y., Feedback Linearization And Linear Stabilization Control of Flexible Robots, Journal of the Chinese Institute of Engineers, Vol. 13, No. 1, 1990, pp. 11-24.

[12] Spong, M. W., Modeling and Control of Robot Manipulators with Elastic Joints, Journal of Dynamic Systems Measurement and Control, Vol. 109, No. 1, 1987, pp. 310-319.

[13] Moberg, S., Hanssen, S., On Feedback Linearization for Robust Tracking Control of Flexible Joint Robots, Proceedings of the 17th World Congress The International Federation of Automatic Control, Seoul, South Korea, 2008, pp. 12218-12223.

[14] Alizadeh, S., Korayem, M. H., and Nekoo, S. R., Design and Implementation of the Output Feedback Linearization Control Method to Determine the DLCC of 6R manipulator, Int J Advanced Design and Manufacturing Technology, Vol. 8, No. 3, 2015, pp. 59-66.

[15] Korayem, M. H., Firouzy, S., Dynamic Load Carrying Capacity of Mobile-Base Flexible link Manipulators: Feedback Linearization Control Approach, International Journal of Robotics, Vol. 3, No. 1, 2013, pp. 34-48.

[16] Cambera, J. C., Chocoteco, J. A., and Feliu, V., Feedback Linearizing Controller for a Flexible Single-Link Link under Gravity and Joint Friction, First Iberian Robotics Conference, Advances in Intelligent Systems and Computing, Springer, Vol. 253, 2014, pp. 169-184.

[17] Jaun, C. C., Vicente, F. B., Input-State Feedback Linearization Control of a Single-Link Flexible Robot Link Moving Under Gravity and Joint Friction, Robotics and Autonomous Systems, Vol. 88, 2017, pp. 24–36.

[18] Yeungs, K. S., Chens, Y. P., Regulation of a One-Link Flexible Robot Link Using Sliding-Mode Technique, International Journal of Control, Vol. 49, No. 6, 1989, pp. 1965-1978.

[19] Hisseine, D., Lohmann B., Robust Control for a Flexible-Link Manipulator Using Sliding Mode Techniques and Nonlinear Control Design Methods, Proceedings of IEEE the International Conference on Robotics & Automation Seoul, South Korea, 2001, pp. 21-26.

[20] Piltan, F., Sulaiman, N., Rashidi, M., Tajpeikar, Z., and Ferdosali, P., Design and Implementation of Sliding Mode Algorithm: Applied to Robot Manipulator-A Review, International Journal of Robotics and Automation,Vol. 2, No. 5, 2011, pp. 265-282.

[21] Etxebarria, V., Sanz, A., and Lizarraga, I., Control of a Lightweight Flexible Robotic Link Using Sliding Modes, International Journal of Advanced Robotic Systems, Vol. 2, No. 2, 2005, pp. 103- 110.

[22] Pezhman, A., Rezapour J., and Mahmoodabadi, M. J., An Optimal Hybrid Adaptive Controller Based On the Multi-Objective Evolutionary Algorithm for an Under-Actuated Nonlinear Ball and Wheel System, Journal of Mechanical Science and Technology, Vol. 34, No. 4, 2020, pp. 1723-1734.

[23] Korayem, M. H., Jalali, M., and Tourajizadeh, H., Dynamic Load Carrying Capacity of Spatial Cable Suspended Robot: Sliding Mode Control Approach, Int J Advanced Design and Manufacturing Technology, Vol. 5, No. 3, 2012, pp. 73-81.

[24] Korayem, M. H., Noroozi, M., and Daeinabi, Kh., Sliding Mode Control of AFM in Contact Mode during Manipulation of Nano-Particle, Int J Advanced Design and Manufacturing Technology, Vol. 6, No. 4, 2013, pp. 83-89.

[25] Yang, X., Zhong Z., Dynamics, and Terminal Sliding Mode Control of Two-Link Flexible Manipulators with Non-collocated Feedback, 3rd IFAC International Conference on Intelligent Control and Automation Science, Beijing, China, 2013, pp. 218-223.

[26] Korayem, M. H., Taherifar, M., and Tourajizadeh, H., Compensating the Flexibility Uncertainties of a Cable Suspended Robot using SMC approach, Robotica, 2014, pp. 1 – 21.

[27] Abdul-Adheem, W. R., Kasim I. I., Improved Sliding Mode Nonlinear Extended State Observer based Active Disturbance Rejection Control for Uncertain Systems with Unknown Total Disturbance, International Journal of Advanced Computer Science and Applications, Vol. 7, No. 12, 2016, pp. 80-93.

[28] Peza-Solís, J. F., Silva-Navarro, G., and Castro-Linares, N. R., Trajectory Tracking Control in a Single Flexible-Link Robot using Finite Differences and Sliding Modes, Journal of Applied Research and Technology, Vol. 13, No.1, 2015, pp. 70-78.

[29] Has, Z., Marzuki, M., and Mardiyah, N. A., Two-Link Flexible Manipulator Control Using Sliding Mode Control Based Linear Matrix Inequality, International Conference on Electrical Engineering Computer Science and Informatics, Vol. 190, 2017, pp. 1-9.

[30] Akbari, A. A., Amini, S., Attitude Control of Unmanned Aerial Vehicle Based on Sliding Mode Technique with Parameter Estimation, Int J Advanced Design and Manufacturing Technology, Vol. 10, No. 2, 2017, pp. 49-59.

[31] Rezapour, J., Afzali, P., Rollover Avoidance in Sport Utility Vehicles: a Multi-Criteria Viewpoint, Automotive Science and Engineering Iran University of Science & Technology, Vol. 10, No. 3, 2020, pp. 3357-3368.

[32] Rezapour, J., Sharifi, M., and Nariman-zadeh, N., Application of Fuzzy Sliding Mode Control to Robotic Manipulator Using Multiobjective Genetic Algorithm, International Symposium on Innovations in Intelligent Systems and Applications, Istanbul, Turkey, 2011.

[33] Park, C. W., Robust Stable Fuzzy Control via Fuzzy Modeling and Feedback Linearization with Its Applications to Controlling Uncertain Single-link Flexible Joint Manipulators, Journal of Intelligent and Robotic Systems, Vol. 39, 2004, pp. 137-141.

[34] Ahmad, M. A., Raja Ismail, R. M. T., Ramli, M. S., Zawawi, M. A., and Suid, M.H., Vibration Control Strategy for Flexible Joint Manipulator: A Fuzzy Logic Control Approach, IEEE Symposium on Industrial Electronics and Applications (ISIEA), Penang, Malaysia, 2010, pp. 1-6.

[35] Naderi, D., Ganjefar, S., and Mosadeghzad, M., Optimization Controller and Observer Design of a Reconfigurable Mobile Robot Using Genetic Algorithm and Neural Network, Int J Advanced Design and Manufacturing Technology, Vol. 3, No. 2, 2010, pp 1-16.

[36] Kandroodi, M. R., Mansouri, M., Aliyari Shoorehdeli, M., and Teshnehlab, M., Control of Flexible Joint Manipulator via Reduced Rule-Based Fuzzy Control with Experimental Validation, ISRN Artificial Intelligence, 2012, pp. 1-8.

[37] Ashraf Ahmad, M., Tumari, Z. M., and Kasruddin Nasir, A. N., Composite Fuzzy Logic Control Approach to a Flexible Joint Manipulator, International Journal of Advanced Robotic Systems, Vol. 10, No. 12013, 2013, pp. 1-9.

[38] Bassera, H., Karamib, H., Shamshirbandc, S., Akiba, S., Amirmojahedia, M., Ahmadd, R., Jahangirzadeha, A., and Javidniae, H., Hybrid ANFIS–PSO Approach for Predicting Optimum Parameters of a Protective Spur Dike, Applied Soft Computing, Vol. 30, 2015, pp. 642–649.

[39] Ghazali, M. R., Ibrahim, Z., Saealal, M. S., and Suid, M. H., Single Input Fuzzy Logic Controller for Flexible Joint Manipulator, International Journal of Innovative Computing, Information and Control, Vol. 1, No. 12, 2016, pp. 181-191.

[40] Mahmoodabadi, M. J., Taherkhorsandi, M., Optimal Robust Design of Sliding-mode Control Based on Multi-Objective Particle Swarm Optimization for Chaotic Uncertain Problems, Int J Advanced Design and Manufacturing Technology, Vol. 10, No. 3, 2017, pp. 115-126.

[41] Hagan, M. T., Menhaj, M., Training Feed-Forward Networks with the Marquardt Algorithm, IEEE Transactions on Neural Networks, Vol. 5, No. 6, 1999, pp. 989–993.

[42] Marquardt, D., An Algorithm for Least-Squares Estimation of Nonlinear Parameters, SIAMJournal on Applied Mathematics, Vol. 11, No. 2, 1963, pp. 431–441.

[43] Jang, J., Yh-Shing, R., Fuzzy Modeling Using Generalized Neural Networks and Kalman Filter Algorithm, Proceedings of the 9th National Conference on Artificial Intelligence, Vol. 2, No. 14–19, 1991, pp. 762–767.

[44] Andalib Sahnehsaraei, M., Mahmoodabadi, M. J., Taherkhorsandi, M., Castillo-Villar, K. K., and Mortazavi Yazdi, S. M., A Hybrid Global Optimization Algorithm: Particle Swarm Optimization in Association with a Genetic Algorithm, Complex System Modelling and Control Through Intelligent Soft Computations, Springer, 2015, pp. 45-86.